Electron Beam Characteristics and Dose Profiles of 9 MeV Varian Clinac 2100C/D Linear Accelerator Using OMEGA BEAMnrc Code System

***Ibrahim. E. Othman[1], Rania Saad Khalifa[2] and Amina Elsariti[3]**
[1]Department of Radiology, Faculty of Medical Technology, Aljufra University.
[2]National Health Service, Libyan Ministry of Health.
[3]Department of Medical Physics, Misurata University
*Corresponding author: ibrahim.othman@ju.edu.ly

Submission date 21 . 2.2022 Acceptance date 28. 2 .2022 Electronic publishing date: 4.12.2022

Abstract: Treatment planning using Monte Carlo (MC) code is widely used to improve different equipments used in radiation therapy. This real simulation technique is becoming more practical in Medical Physics, particularly with the rapid development of computer technology. Such simulation requires accurate detailed knowledge of radiation beams as well as the accurate construction of medical linear accelerators (Linacs). In the present work the dosimetric properties of 9-MeV electron beam of the Varian Clinac 2100C/D Linac were investigated. The dosimetric features of interest are, the central-axis absorbed dose, the beam profiles, the photon, electron and positron fluences and energy fluences, the mean energy, the spectral distribution, and the isodose curves. The above mentioned Linac was simulated using OMEGA BEAMnrc MC code system to produce 10x10cm phase space of electron beam. The detailed spectra of the phase-space files resulted from the present simulation and that provided by the International Atomic Energy Agency (IAEA) for the electron beam of 10cmx10cm field of view were modeled, simulated and finally analysed using BEAMdp. The central axis depth-dose curves, dose profiles and isodose curves of the electron beams in water phantom were also scored and analysed using DOSXYZnrc, STATDOSE and DOSXYZ_SHOW code. This study demonstrates that the MC code system can create the phase space data files which can be used to generate accurate MC dose distributions for electron beams produced using clinical high energy Linacs in water phantom or in patients for the sake of radiation therapy.

Keywords: Medical Physics, Radiation Dosimetry, Linear Accelerators, Monte Carlo OMEGA BEAMnrc, Phase Space File, Dose Profiles, Isodose Curves

1. Introduction:

Radiation therapy (RT) methods are used to treat the cancer. The patient's tumour is exposed to ionizing radiation [1]. RT can either be used on its own or combined with surgery or chemo-therapy [2]. In external beam radiotherapy (EBRT), the source of radiation is delivered from outside of the patient. EBRT generally requires a computerized treatment plan to ensure accurate dose delivery to the desired target and to ensure adequate sparing of any organs at risk (OAR) [3]. Typically, a patient will be scanned at a computed tomography (CT) simulator to obtain a three-dimensional (3D) image for definition of the target and OAR [1]. In the treatment planning stage, both the target and OAR are delineated on the 3D image [3]. The arrangement of beam is selected so that the dose coverage to the target tumor is maximised while the dose to the OAR is minimised. A deterministic dose calculation algorithm, such as convolution-superposition, simulates this process [3]. Varian linear accelerators (Palo Alto, CA) are often accom-panied by the Varian EclipseTM treatment planning system, which uses the AAA convolution-superposition algorithm [4]. It is necessary for dose calculation algorithms to have high accuracy to deliver the desired dose distribution to the patient very accurately [5].

Tumors can be treated with a single field from the front, a single field from the back or with two fields from the opposite sides. This is called conventional EBRT where the combination of fields helps to uniformly deliver dose across the tumor. Sometimes 3 or 4 fields are used. Using arc therapy, the gantry of the linear accelerator may rotate during the treatment. In the 3-D Conformal Radiation Therapy, enhanced imaging technology of the body allows for programming of treatment beams. This technique conforms better to the shape of a tumor. By treating with large numbers of beams each shaped with a Multi Leaf Collimator (MLC), radiation dose is delivered uniformly and conformally to the tumor. In recent years, the Intensity Modulated Radiation Therapy (IMRT) is considered as one of the latest advancements in radiation therapy. This new approach allows for dose sculpting and even distribution of delivery for precise uniform treatment. In this technique, the MLC moves and modulates the radiation as the linac treats the patient [6-10]. In previous studies, we presented that, for EBRT and Brachytherapy, Monte Carlo Electron Gamma Shower (EGSnrc) maintained by National Research Council of Canada (NRCC) along with its different tools has showed its advancements in dose calculations in general and

radiotherapy planning in particular [11-14]. In the present work, the main objective is to, first, simulate the Varian Clinac 2100C/D Linac to produce the phase space file at 100 cm Source to Surface Distance (SSD), just above either the patient or the phantom surface, using BEAMnrc code. The phase space file is a collection of representative pseudo-particles emerging from a radiation therapy treatment source along with their properties that include particle type, energy, position, direction, progeny and statistical weight. Analysis of the phase space were done using BEAMDP code. Second, calculations of the transmitted dose in the water phantom are investigated. Phase space file that resulted from the present simulation and that provided by the International Atomic Energy Agency IAEA are investigated for accuracy checkup. The Monte Carlo code system BEAMnrc and DOSXYZnrc were used to model the high energy electron linac head and to calculate the transmitted dose in the water phantom. Analysis of the data and isodose curves were done using, STATDOSE and DOSXYZ_SHOW codes.

2. Monte Carlo in Radiation Therapy

The Monte Carlo code system used in this study was the latest, year v2021 release, of general purpose Fortran-based BEAMnrc code package maintained by National Research Council of Canada (NRCC) [15,16]. The dose calculation in water phantom is carried out with DOSXYZnrc package associated with BEAMnrc code system [17]. All these code packages used here as well as other different codes are based on the simulation of coupled electron-photon transport EGSnrc code system and maintained by NRCC [18]. The code system was installed on Intel quadrupole processor running Debian GNU Linux workstation along with the GNU compilers suite. The geometry models were based on electron beam from Varian Clinac 2100C/D medical linear accelerator. Common components in the geometry model for the beams are: primary collimator, vacuum exit window, dual ionization chamber, lead shielding plate, field mirror with its frame, jaws, fully retracted multileaf collimator and light field reticle. Above primary collimator there is a two-layer x-ray target in photon beam and vacuum in electron beam. Between vacuum exit window and dual ionization chamber there is a flattening filter in photon beam and dual scattering foils in electron beam. Below light field reticle there is air to the level of phantom surface, but in electron beam there is an electron applicator with square Cerrobend™ cut-out. In electron beam model the nominal energy is 9MeV. The particle data is gathered to phase space files at 100 cm source to surface distance (SSD). In electron beam model the electron applicator size produces 10x10 cm2 field at 100 cm SSD. The EGSnrc parameters are: ECUT=AE=0.521 MeV, PCUT=AP=0.01 MeV, Electron-step algorithm=PRESTA-II, Spin effects=On, Brems angular sampling=KM, Brems cross sections=NIST, Bound Compton scattering= On, Pair angular sampling=KM, Photoelectron angular sampling=KM, Rayleigh scattering=On, Atomic relaxations=On, Electron impact ionization = On and Photon cross sections=xcom. The phantom simulations were performed with DOSXYZnrc. The phase space data are used as input. For electron beam the number of histories is $5x10^8$. The sizes of calculation voxels were adapted to be small in regions of high dose gradients and vice versa. In horizontal plane (X-axis) sizes varied between 0.2 to 1 cm in electron beam model, being the smallest near "profile shoulder" and penumbral region. The horizontal voxels around beam central axis were combined to larger voxels to produce statistically more reliable calculation results. In vertical direction (Z-axis) sizes varied between 0.1 to 1.0 cm, being the smallest near the surface, in dose build-up region, around the depth of dose maximum (d_{max}) and in the end of linear dose build-down region. Statistical uncertainties for the calculated dose values for each voxel were below 0.002 %, being slightly higher near the surface in Z axis and in the ends of profiles. The EGSnrc parameters are the same as in first phase simulations. Calculated vertical dose distributions were normalized to percentage depth dose (PDD) curves and also to unity. In Monte Carlo simulation of high energy medical linear accelerators (Linacs), important components are to be controlled in order to shape the output beam [10-13].

3. Results and Discussions

The IAEA phase space file at 100 cm SSD and 10x10cm field of view for Varian Clinac 2100C Linac using BEAMdb was investigated. Beam characteristics; particle and energy fluence, spectral and angular distribution, and mean energy data of electrons, positrons, photons and total particles were extracted, analysed and represented to show the following:

Particle Fluence Versus Position

Figure 1 shows the particle fluence versus position x for; all particles (a), electrons (b), positrons (c) and photons (d). All the graphs shows the same trend except that the number of positrons are quite low compared to the number of electrons and photons. This is quite clear from the y-axes scales where the beam is mainly electrons and photons with some positrons scattered from the collimator parts. Notice the high standard deviation in the positron graph due to its poor count rate statistics.

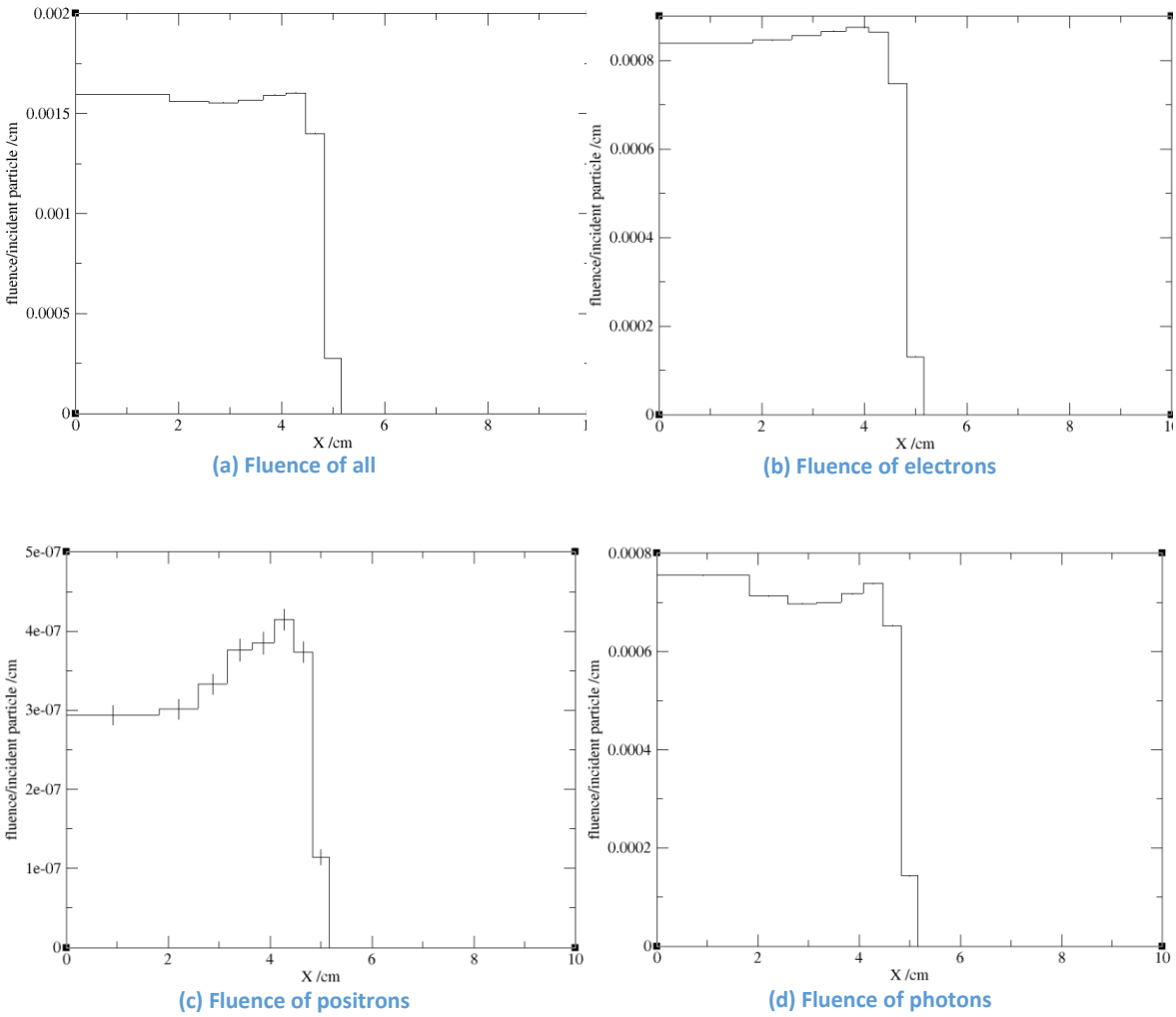

Fig. 1 Total (a), electrons (b), positrons (c) and photons (d) fluence are represented as functions of distance x.

Energy Fluence Versus Position

Figure 2 shows the particle energy fluence versus position x for; all particles (a), electrons (b), positrons (c) and photons (d). All the graphs shows again the same trend except that the number of positrons are quite low compared to the number of electrons and photons. This is quite clear from the y-axes scales where the beam is mainly electrons and photons with some positrons scattered from the collimator parts. Notice the high standard deviation in the positron graph due to its poor count rate statistics.

Energy Fluence Distribution

Figure 3 shows the particle energy fluence distribution for; all particles (a), electrons (b), positrons (c) and photons (d). The energy fluence distribution of electrons is gives peak at energy around 9 MeV while that of both photons and positrons gives peak around 2 MeV. The number of positrons are quite low compared to the number of electrons and photons. This is quite clear from the y-axes scales where the beam is mainly electrons and photons with some positrons scattered from the collimator parts. Notice the high standard deviation in the positron graph due to its poor count rate statistics.

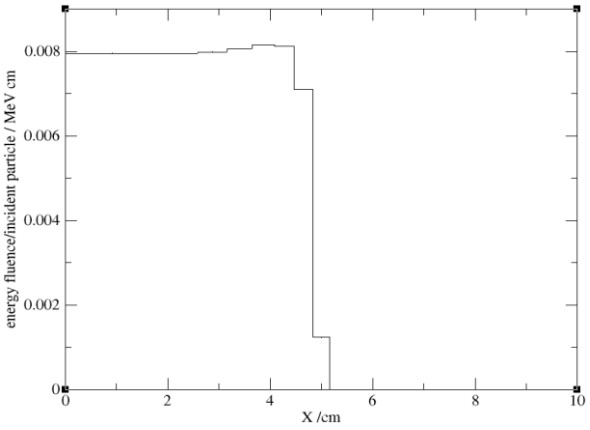

(a) Energy fluence of all

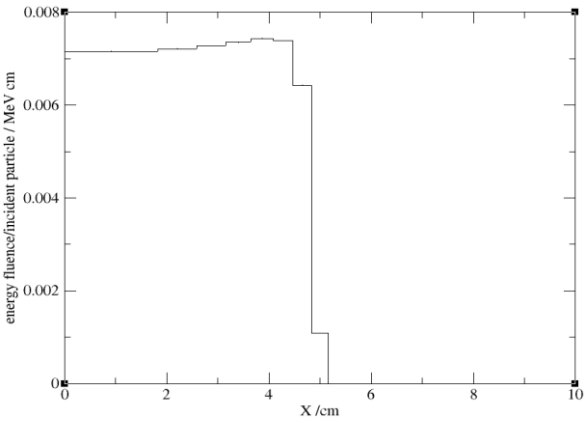

(b) Energy fluence of electrons

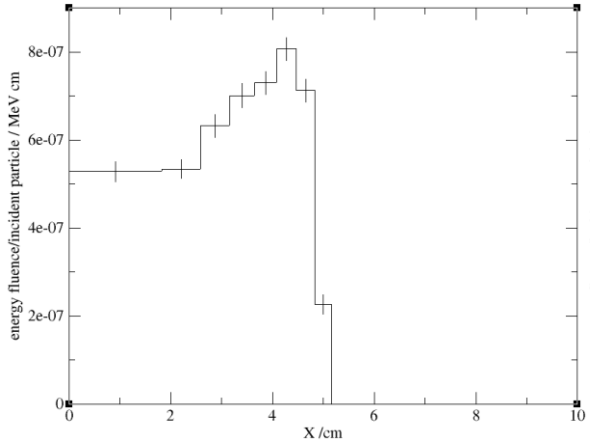

(c) Energy fluence of positrons

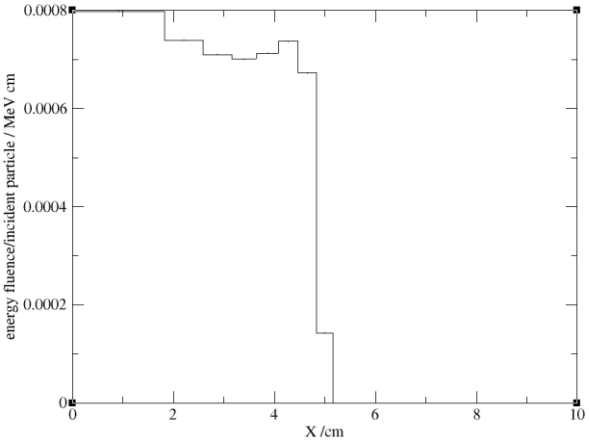

(d) Energy fluence of photons

Fig. 2 Total (a), electrons (b), positrons (c) and photons (d) energy fluence are represented as functions of distance x.

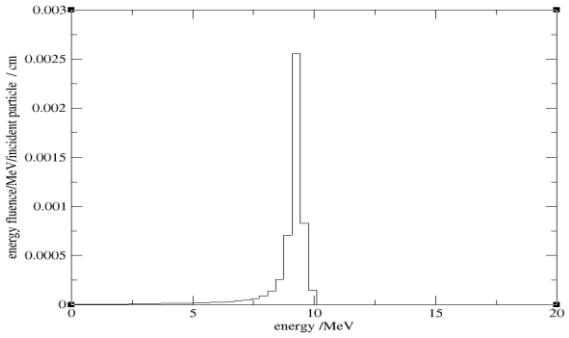

(a) Energy fluence distribution of all

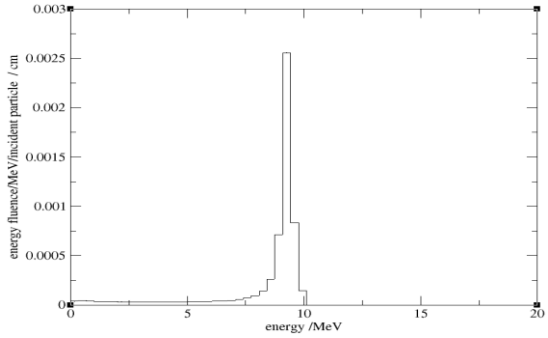

(a) Energy fluence distribution of electrons

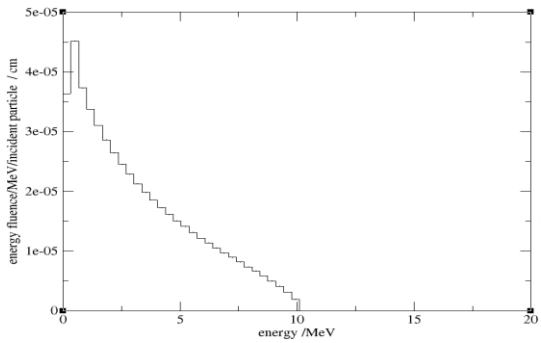

(c) Energy fluence distribution of positrons

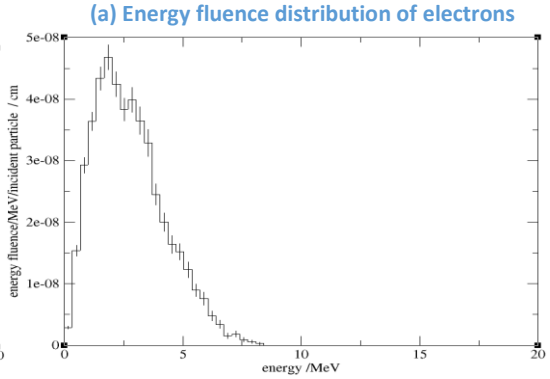

(d) Energy fluence distribution of photons

Fig. 3 Total (a), electrons (b), positrons (c) and photons (d) energy fluence distribution are represented as functions of energy bins

Angular Distribution

Figure 4 shows the particle angular distribution for; all particles (a), electrons (b), positrons (c) and photons (d). All the particles where scored in solid angular bins and the graphs do not show the same trend where there are a number of positrons are scattered by the collimator parts with angles sometimes reach 30°-40° compared to about 4° angles of electrons and photons.

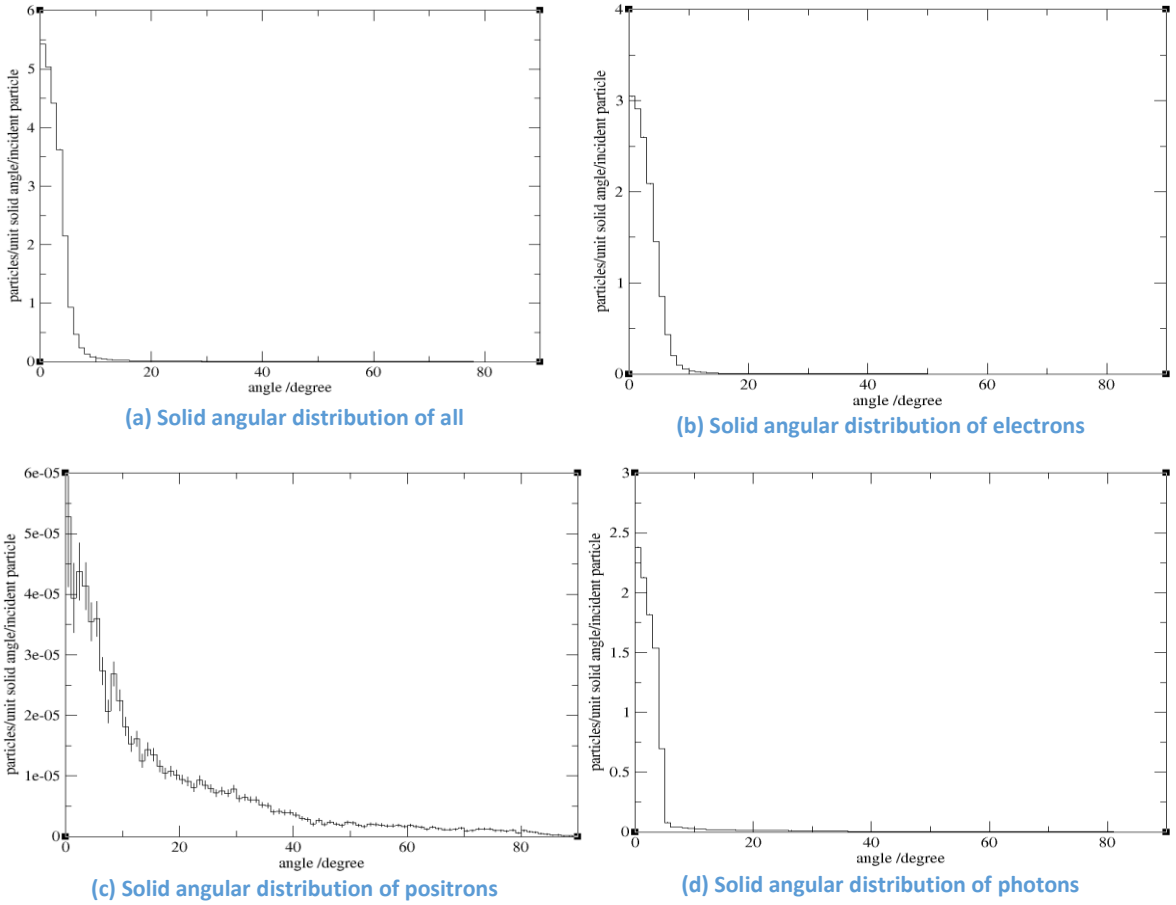

(a) Solid angular distribution of all

(b) Solid angular distribution of electrons

(c) Solid angular distribution of positrons

(d) Solid angular distribution of photons

Fig. 4 Total (a), electrons (b), positrons (c) and photons (d) angular distribution are represented as functions of solid angle in degrees.

Mean Energy Distribution

Figure 5 shows the particle mean energy versus position x for; all particles (a), electrons (b), positrons (c) and photons (d) where the mean energy is about 8.5 MeV for electrons, 1.9 MeV for positrons and 1 MeV for photons and it is highest at the centre of the beam with radius about 5cm for all particles.

Spectral Distribution

The phase space file was used to obtain the spectral distribution of 10cmx10cm field of view beam as shown in Figure 6. The figure shows that the electrons are the main component of the beam and the least are the positrons. The less is the number of positrons in the produced beam, the higher is the scattering of points of the spectral curve. This is due to the poor statistics of the very small number of positrons. This is expected for an electron beam of any linear accelerator because of the interactions of the emerging x-ray photons with the collimators. The spectral peak maximum is around 9 MeV for electrons and around 1-2 MeV for positrons and photons.

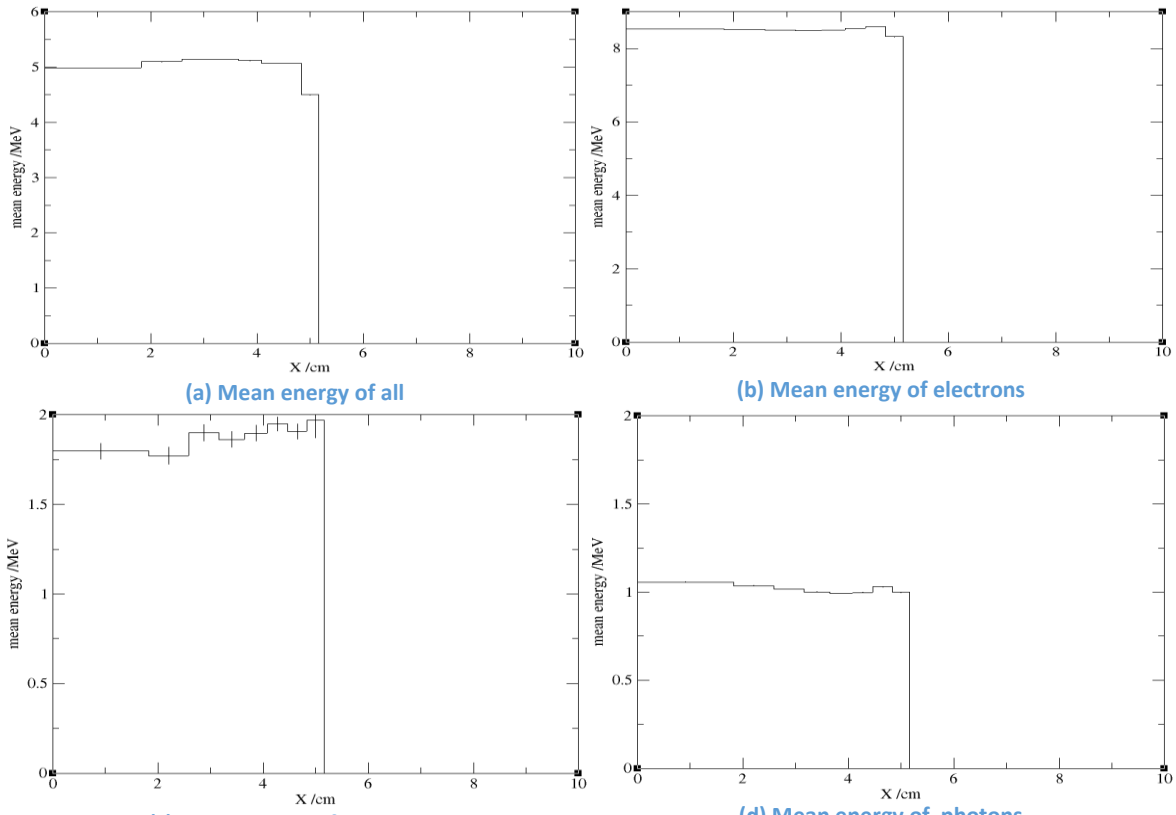

(a) Mean energy of all

(b) Mean energy of electrons

(c) Mean energy of positrons

(d) Mean energy of photons

Fig. 5 Total (a), electrons (b), positrons (c) and photons (d) mean energy are represented as functions of distance x

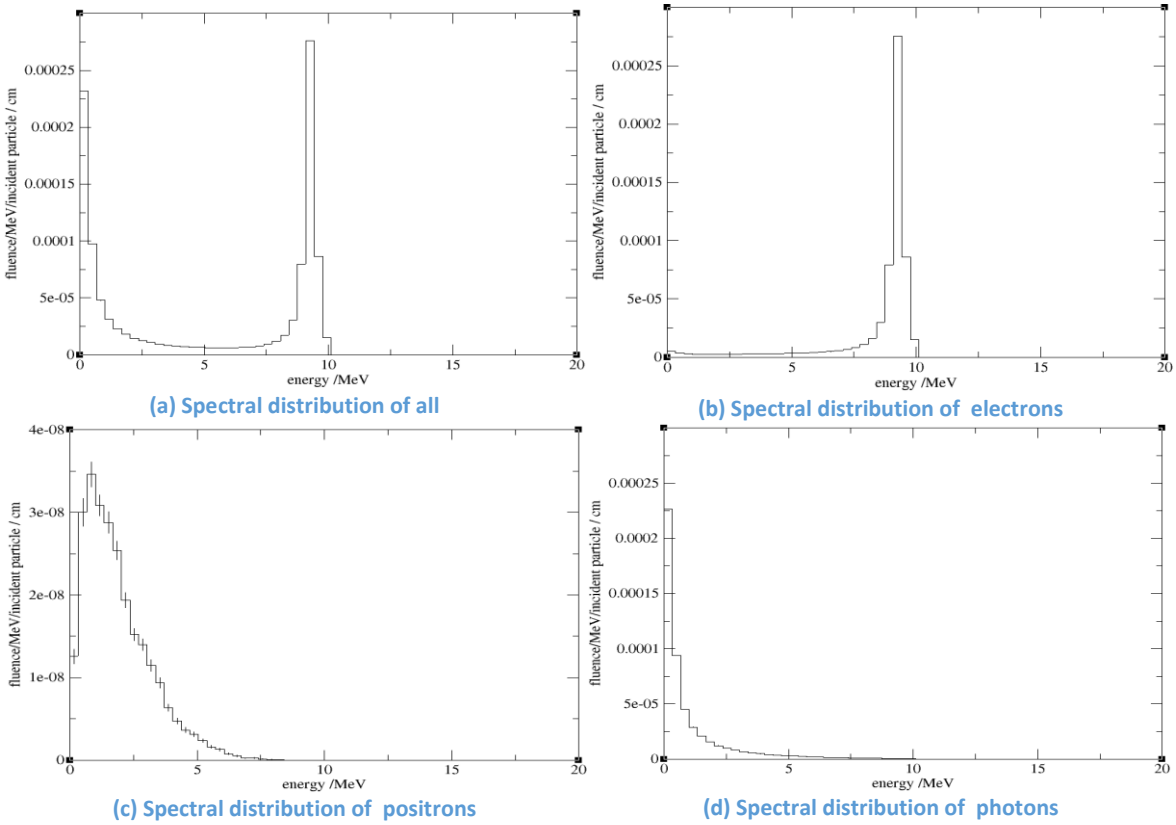

(a) Spectral distribution of all

(b) Spectral distribution of electrons

(c) Spectral distribution of positrons

(d) Spectral distribution of photons

Fig. 6 Total (a), electrons (b), positrons (c) and photons (d) spectral distribution are represented as functions of energy bins.

Off-Axis Ratios (OAR) And Beam Profiles

Dose distributions along the beam central axis give only part of the information required for an accurate dose description inside the patient. Dose distributions in two (2-D) and three (3-D) dimensions are determined with central axis data in conjunction with off-axis dose profiles. Combining a central axis dose distribution with off-axis data results in a volume dose matrix that provides 2-D and 3-D information on the dose distribution. The off-axis ratio (OAR) is usually defined as the ratio of dose at an off-axis point to the dose on the central beam axis at the same depth in a phantom. As in the present work, megavoltage beam profiles consist of three distinct regions: central, penumbra and umbra. The central region represents the central portion of the profile extending from the beam central axis to 5cm in this study as illustrated in figure 7(b). In the penumbral region of the dose profile the dose changes rapidly and depends also on the field defining collimators. Umbra is the region outside the radiation field, far removed from the field edges which is beyond 5cm in this study. The IAEA phase space file of Varian 9MeV 2100C/D Clinac linear accelerator was used to score the depth dose distribution curves in water phantom at 100cm SSD using the DOSXYZnrc code system. The beam field of view is 10x10cm. The data were analysed and presented using STATDOSE code with the aid of Grace software. Figure 7(a) shows the dose curves at four different xy plane areas in the direction off the central axis where the depth is set in the z-direction. The maximum dose D_{max} moves toward higher depths as the xy area increases. Figure 7(b) shows the dose profile of the beam around the central axis. It shows the dose fall off at 5cm on either side which is the radius of the 10cmx10cm field of view of the photon beam.

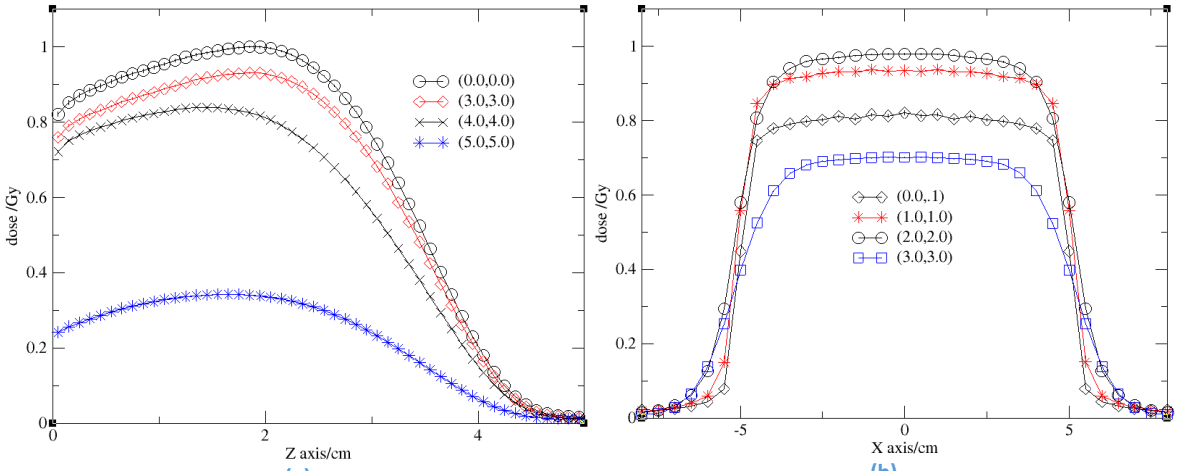

Fig. 7 Depth dose distribution of 10cmx10cm photon beam in water phantom (a) and dose profile of the central beam (b)

Isodose Curves:

The data of the central axis depth doses combined with the dose profiles gives complete 2-D and 3-D information about a radiation beam. This information is difficult to visualize. Planar and volumetric variations in depth doses are usually displayed by means of isodose curves or isodose surfaces, which connect points of equal dose in a volume of interest to represent the so-called dose contour. The isodose curves and surfaces are usually drawn at regular intervals of absorbed dose and are expressed as a percentage of the dose at a specific reference point. An isodose chart for a given single beam consists of a family of isodose curves usually drawn at regular increments of Percentage Depth Dose (PDD).

The dose then could be normalized in either Source to Surface Distance set-up (SSD) or in Source to Axis Distance (SAD) set-up. In the present work, the DOSXYZ_SHOW software was used to display the dose data with the created water phantom file during the simulation. Figure 8 shows the isodose charts for Varian 9MeV 2100C/D Clinac linear accelerator electron beam in water phantom. It shows an SSD set-up (A = 10 × 10 cm^2; SSD = 100 cm). Figure 8(a) shows xz planner view while figure 8(b) is the xy planner view. The coordinate cross markers in both figures can move everywhere at any position on the image to display the dose information at the top of the images. The isodose curves show that near the beam edges in the penumbra region, the dose decreases rapidly with lateral distance from the beam central axis. This dose fall-off is apparently caused by both the geometric penumbra effect and the reduced side scatter. In

umbra region outside the radiation field, far removed from the field edges which is beyond 5cm in this study, the dose is decreased to a minimum.

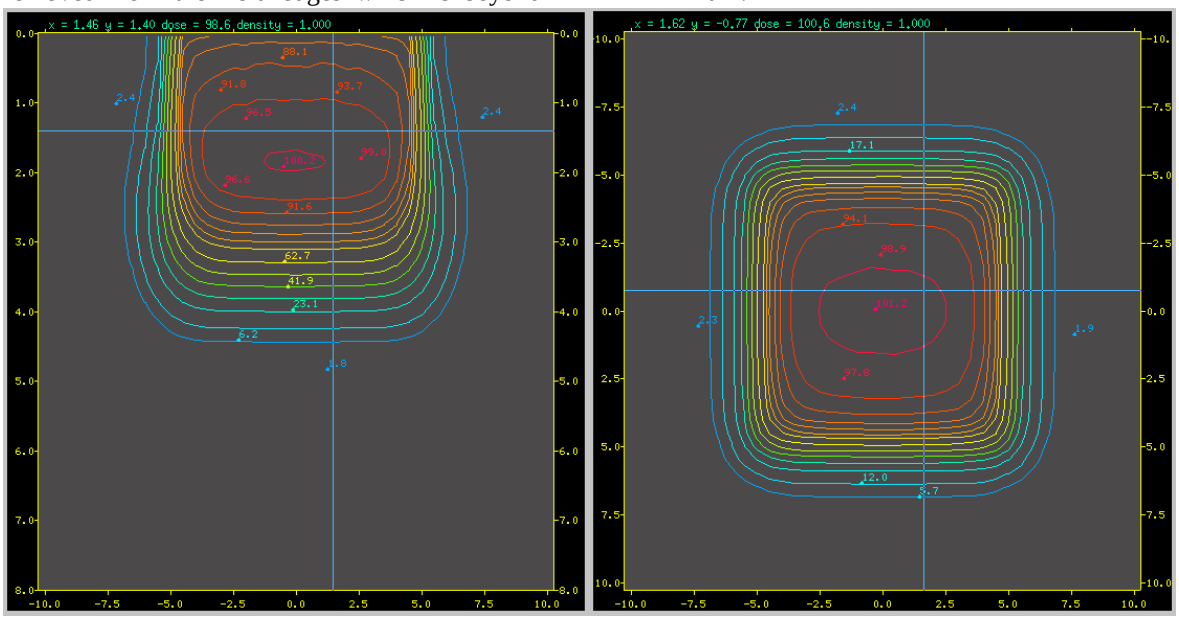

(a) (b)

Fig. 8 Isodose charts for Varian 9MeV 2100C/D Clinac Linac electron beam in water phantom. It shows an SSD set-up (A = 10 × 10 cm2; SSD = 100 cm). It shows xz (a) and xy (b) planner view.

Conclusion

The Monte Carlo MC code OMEGA BEAM was used to simulate the Varian 9MeV 2100C/D Clinac Linac using BEAMnrc photon beam linear accelerator. The accelerator beam spectra at 100cm source to surface distance SSD were produced and analyzed. The depth dose curves and dose profiles for 10cmx10cm field of view beam were scored in water phantom. Planar and volumetric variations in depth doses were displayed by means of isodose curves or isodose surfaces, which connect points of equal dose in a volume of interest to represent the so-called dose contour. OMEGA BEAM code proved to be capable and accurate for radiotherapy treatment planning. The dose profiles were represented in a SSD set-up (A = 10 × 10 cm^2; SSD = 100 cm). The isodose curves show that at 5cm near the beam edges in the penumbra region, the dose decreases rapidly with lateral distance from the beam central axis. This dose fall-off is apparently caused by both the geometric penumbra effect and the reduced side scatter. In umbra region outside the radiation field, far removed from the field edges which is beyond 5cm in this study, the dose is decreased to a minimum.

References:

[1] International Atomic Energy Agency, Radiation Oncology Physics: A Handbook for Teachers and Students, E.B. Podgorsak, Ed. Vienna: IAEA, 2005.

[2] R. Baskar, K. Lee, R. Yeo, and K. Yeoh, "Cancer and Radiation Therapy: Current Advances and Future Directions," Int. J. Med. Sci. 9, 193-199 (2012).

[3] B. Fraass et al., "American Association of Physicists in Medicine Radiation Therapy Committee Task Group 53: Quality assurance for clinical radiotherapy treatment planning," Med. Phys. 25, 1773-1829 (1998).

[4] J. Sievinen, W. Ulmer, W. Kaissl. AAA photon dose calculation model in Eclipse. Palo Alto (CA): Varian Medical Systems; 2005

[5] A. Ahnesjö and M. Aspradakis, "Dose calculations for external photon beams in radiotherapy," Phys. Med. Biol. 44, R99-R155 (1999).

[6] H. Johns and J. Cunningham (1983). "The Physics of Radiology." (4th edition).

[7] J. Van (1999). "The Modern Technology of Radiation Oncology – A Compendium for Medical Physicists and Radiation Oncologists." Medical Physics Publishing.

[8] F. Khan (2003). "The Physics of Radiation Therapy." Lippincott Williams & Wilkins(3 edition).

[9] L. Vazquez- Quino et al "Monte Carlo modeling of a Novalis TX Varian 6 MV with HD-120 multileaf collimator" J Applied Clinical Med Phys, 13(5), 2012

[10] J. Yang , Li J, L. Chen , R. Price, S McNeeley, L Qin, et al. Dosimetric verification of IMRT treatment planning using Monte Carlo simulations for prostate cancer. Phys Med Biol 2005;50(5):869–78.

[11] I. Othman, B. Abour, Z. Alsnosi. Non-Uniform Spatial Dose Distributions Around Co-60 in Human Tissue for Brachytherapy Treatment using Monte Carlo EGS Code. Alq J Med App Sci. 2022;5(2):396-405. https://doi.org/10.5281/zenodo.6892393

[12] I. Othman and M. Amer. Non-Uniform Spatial Dose Distributions Around Ir-192 for Treating Oral Cavity in Brachytherapy using Monte Carlo EGS Code, ICTS2019, 4-6 March 2019

[13] I. Othman, M. Elgemaey. A study of Photon Beam Characteristics, Dose Profiles and Isodose curves of 6 MV Varian Clinac 600C Linear Accelerator Using OMEGA BEAMnrc Monte Carlo Code System, 14 th Arab Conference on the Peaceful Uses of Atomic Energy, Sharm El-Sheikh, Arab Republic of Egypt, 16 - 20 December 2018

[14] I. Othman, S.. Abuzariba and R. El-Doppati, Radiotherapy Treatment Planning of 16 MV X-Ray Linear Accelerator Using OMEGA BEAMnrc Monte Carlo Code System, The First Annual Conference on Theories and Applications of Basic and Biosciences, 2017, 331-337

[15] D. Rogers et al. (2007). "BEAMnrc User's Manual." Report PIRS 0509.

[16] D. Rogers, B. Faddegon, et al. (1995). "BEAM: a Monte Carlo code to simulate radiotherapy treatment units." Med Phys 22 (5): 503-24.

[17] D Rogers, B. Walters, et al. (2004). "DOSXYZnrc User's Manual." Report PIRS 794.

[18] I. Kawrakow, E. Mainegra-Hing, D. Rogers, F. Tessier, B. Walters. The EGSnrc Code System: Monte Carlo Simulation of Electron and Photon Transport. NRCC Report PIRS-0701. 2009. p. 310.